

Electronic Supplementary Information

Article Title: Two-dimensional Magnetic Metal-Organic Frameworks with Shastry-Sutherland Lattice

Li-Chuan Zhang, ^{†abc} Lizhi Zhang, ^{†d} Guangzhao Qin,^e Qing-Rong Zheng,^f Ming Hu, ^{*e} Qing-Bo Yan^{*a} and Gang Su^{*fg}

^a Center of Materials Science and Optoelectronics Engineering, College of Materials Science and Optoelectronic Technology, University of Chinese Academy of Sciences, Beijing 100049, China

^b Peter Grünberg Institut and Institute for Advanced Simulation, Forschungszentrum Jülich and JARA, 52425 Jülich, Germany

^c Department of Physics, RWTH Aachen University, 52056 Aachen, Germany

^d Department of Physics and Astronomy, University of Tennessee, Knoxville, Tennessee 37916, United States

^e Department of Mechanical Engineering, University of South Carolina, Columbia, SC 29208, USA

^f School of Physics, University of Chinese Academy of Sciences, Beijing 100049, China

^g CAS Center for Excellence in Topological Quantum Computation, and Kavli Institute for Theoretical Sciences, University of Chinese Academy of Sciences, Beijing 100190, China

Table of Contents

| | |
|--|----|
| Electronic Supplementary Information..... | 1 |
| 1. Supplemental calculation details..... | 3 |
| 1.1 Definition of binding energy..... | 3 |
| 1.2 The calculation of U_{eff} | 3 |
| 2. Geometric structure of TM-PBP..... | 5 |
| 2.1 From TM-PBP framework to Shastry-Sutherland (SS) lattice..... | 5 |
| 2.2 The geometric parameters of TM-PBP frameworks..... | 5 |
| 3. Magnetic configurations of TM-PBP..... | 6 |
| 4. Electronic structures of TM-PBP..... | 7 |
| 4.1 Band structures of TM-PBP (TM=Cr, Fe, Co, Ni, Cu, Zn)..... | 7 |
| 4.2 PDOS of AFM Co-PBP and NM Cu-PBP..... | 8 |
| 4.3 Spin-polarized charge density distribution of TM-PBP..... | 9 |
| 5. 2D Ising model for SS lattice..... | 10 |
| 5.1 2D Ising Hamiltonian for SS lattice..... | 10 |
| 5.2 The calculation of exchange coupling constants J_1 and J_2 | 10 |
| 5.3 Spin wave dispersion of Mn-PBP..... | 11 |
| 6. The influence of the different effective U | 12 |
| 6.1 Magnetic ground state of Mn-PBP with different U_{eff} | 12 |
| 6.2 The band structures of Mn-PBP with different U_{eff} | 13 |
| 6.3 The simulated Curie temperature of Mn-PBP with different U_{eff} | 14 |
| 7. Strain effects on the electronic structure of Mn-PBP..... | 15 |
| 8. Magnetic anisotropic energy..... | 16 |
| 9. Mn-PBP under compression..... | 17 |

1. Supplemental calculation details

1.1 Definition of binding energy

The binding energy between TM atoms and PBP molecules is defined as follow,

$$E_{binding} = \frac{2 \times E_{PBP} + 4 \times E_{TM} - E_{TM-PBP}}{4} \quad (1)$$

where the E_{TM-PBP} represents the total energy of a single unit cell of TM-PBP, which contains 2 PBP molecules and 4 TM atoms. Thus $E_{binding}$ can be considered as the binding energy per TM atom.

1.2 The calculation of U_{eff}

To confirm the FM ground state of Mn-PBP, the linear response theory (LRT) was adopted to calculate the value of U_{eff} . The Hubbard U can be calculated as follows:

$$U = \frac{\partial E[\{q_i\}]}{\partial q_i^2} - \frac{\partial E^{KS}[\{q_i\}]}{\partial q_i^2} \quad (2)$$

where q_i represents the d state occupations in i atom, $E[\{q_i\}]$ is the occupation-dependent energy function which is required for the self-consistent solution of the non-interacting Kohn-Sham equations and $E^{KS}[\{q_i\}]$ represents the occupation-dependent energy function.

We use

$$\alpha_i = -\frac{\partial E[\{q_i\}]}{\partial q_i} \quad \alpha_i^{KS} = -\frac{\partial E^{KS}[\{q_i\}]}{\partial q_i} \quad (3)$$

where α_i represents the localized perturbation potential shift in i atom.

$$U = \frac{\partial \alpha_i^{KS}}{\partial q_i} - \frac{\partial \alpha_i}{\partial q_i} = (\chi_0^{-1} - \chi^{-1})_i \quad (4)$$

where χ_0 and χ represent the non-interaction and interaction density response functions of the system with respect to the localized potential shift, respectively. The calculation was performed using the Quantum Espresso code with the GGA (PBE) exchange-correlation function and PAW pseudopotential.

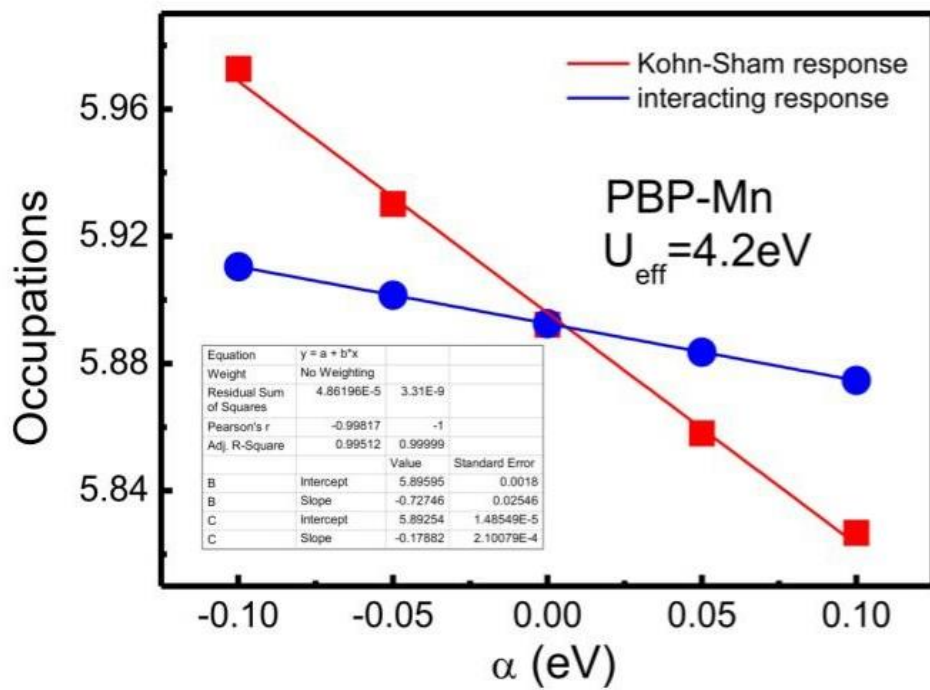


Figure S1. The interacting occupations and Kohn-Sham occupations versus localized perturbation potential shift for PBP-Mn. The U_{eff} of PBP-Mn can be derived as 4.2 eV.

2. Geometric structure of TM-PBP

2.1 From TM-PBP framework to Shastry-Sutherland (SS) lattice

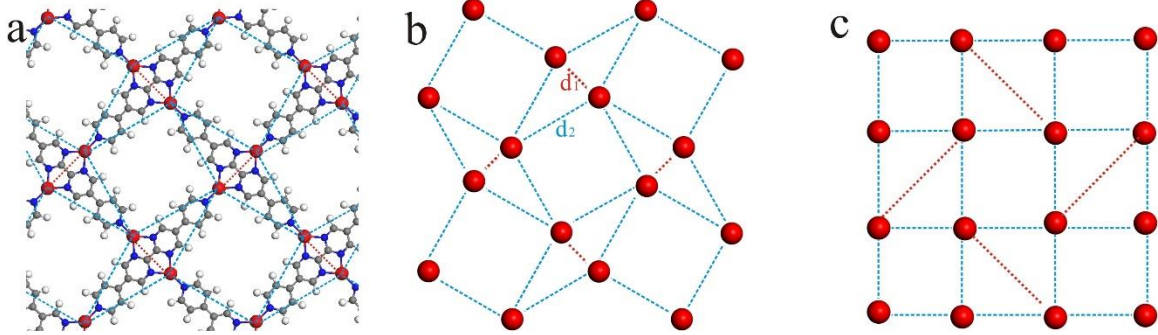


Figure S2. (a) TM-PBP schematic structure. The red balls indicate the TM atoms. (b) The abstraction of (a) by focusing on TM atoms. The red dot lines (d_1) and blue dashed lines (d_2) represent the interactions between the nearest TM atoms and the second nearest TM atoms, respectively. (c) The conventional standard Shastry-Sutherland lattice, which is topologically-equivalent to (b).

2.2 The geometric parameters of TM-PBP frameworks

Table S1. The geometric parameters of TM-PBP frameworks. a (\AA) represents the length of the unit cell; d_1 (\AA) and d_2 (\AA) are on behalf of the distance between the nearest TM atoms and second nearest TM atoms, respectively; TM-N1 (\AA) and TM-N2/3(\AA) represent the distances of TM atom and its nearby N atoms separately; N1-TM-N2/3 and N2-TM-N3 indicate the angles formed by corresponding atoms, respectively.

| | a | d_1 | d_2 | TM-N1 | TM-N2/3 | N1-TM-N2/3 | N2-TM-N3 |
|-----------|-------|-------|-------|-------|---------|------------|----------|
| <i>Cr</i> | 18.17 | 5.91 | 10.33 | 2.10 | 2.22 | 141.91° | 76.18° |
| <i>Mn</i> | 17.79 | 5.50 | 10.21 | 2.01 | 2.06 | 138.18° | 83.64° |
| <i>Fe</i> | 17.67 | 5.43 | 10.15 | 1.97 | 2.03 | 137.72° | 84.57° |
| <i>Co</i> | 17.62 | 5.46 | 10.11 | 1.96 | 2.03 | 138.40° | 83.20° |
| <i>Ni</i> | 17.49 | 5.33 | 10.06 | 1.94 | 1.98 | 137.07° | 85.86° |
| <i>Cu</i> | 17.55 | 5.44 | 10.07 | 1.90 | 2.02 | 137.68° | 84.63° |
| <i>Zn</i> | 17.34 | 5.17 | 10.01 | 1.89 | 1.94 | 135.31° | 89.37° |

3. Magnetic configurations of TM-PBP

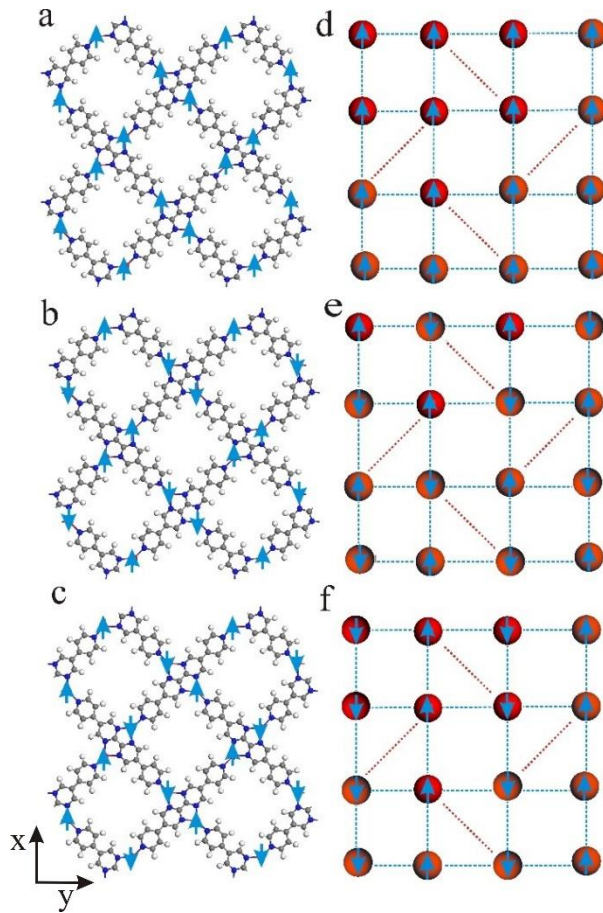


Figure S3. Magnetic configurations of TM-PBP. The upward and downward blue arrows illustrate spin-up and spin-down local magnetic moments (the direction of spin is along z -direction), respectively. (a), (b) and (c) indicate the FM, Néel AFM and stripe AFM configurations for TM-PBP system. (d), (e) and (f) illustrate magnetic configurations of (a), (b) and (c) in the form of conventional standard Shastry-Sutherland lattice, respectively.

4. Electronic structures of TM-PBP

4.1 Band structures of TM-PBP (TM=Cr, Fe, Co, Ni, Cu, Zn)

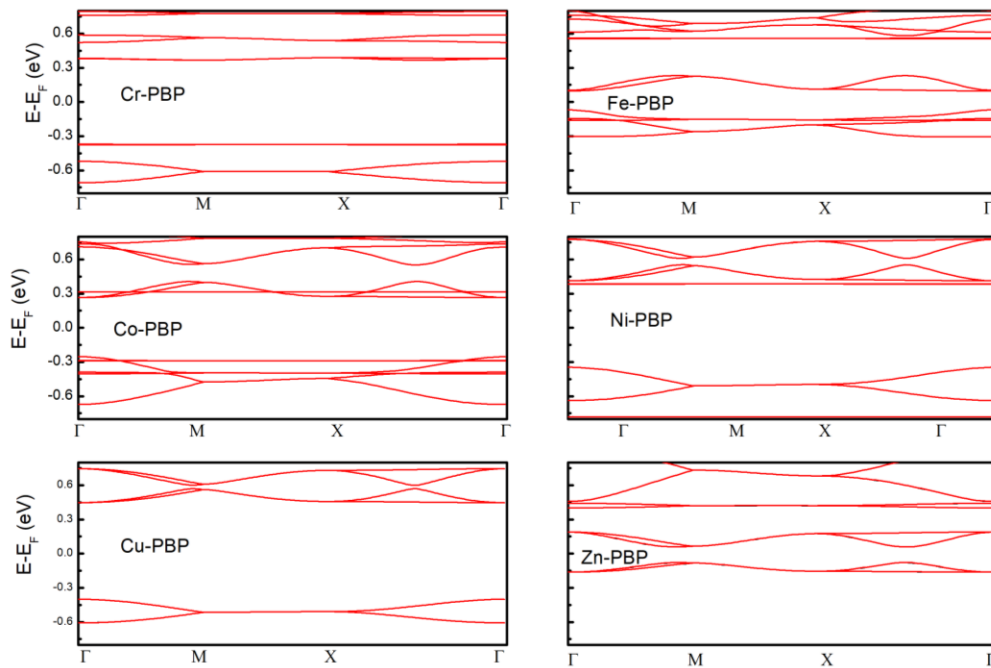


Figure S4. Band structures of TM-PBP (TM=Cr, Fe, Co, Ni, Cu, Zn). For AFM TM-PBP (TM=Cr, Fe, Co, Ni), the spin-up and spin-down energy bands are identical to each other. The GGA+ U method is used and the value of effective U is 3 eV for all calculation.

4.2 PDOS of AFM Co-PBP and NM Cu-PBP

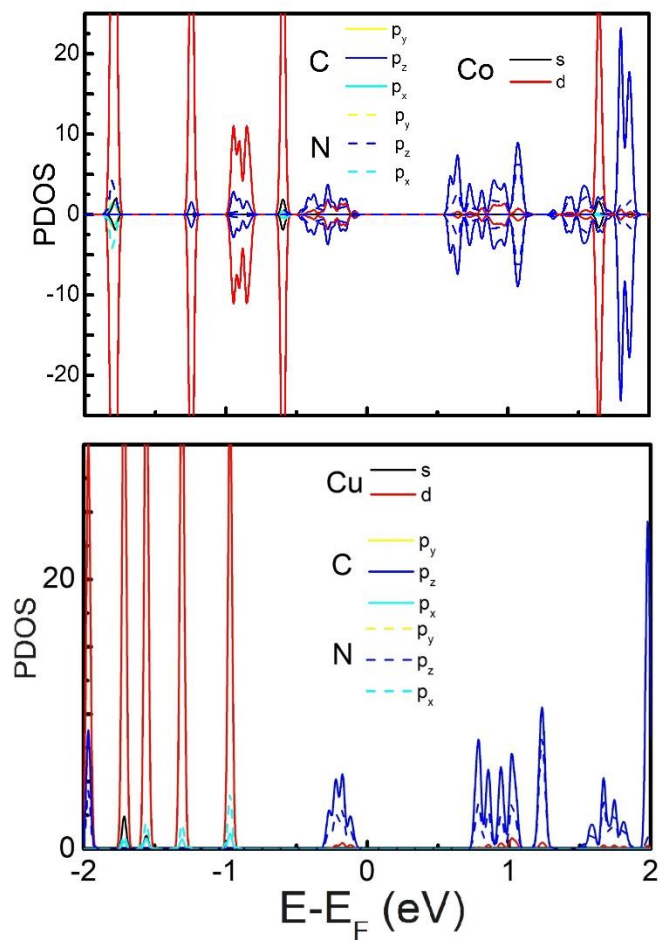


Figure S5. The PDOS of (a) Co-PBP and (b) Cu-PBP. The GGA+U method is used and the value of effective U is 3 eV for all calculation.

4.3 Spin-polarized charge density distribution of TM-PBP

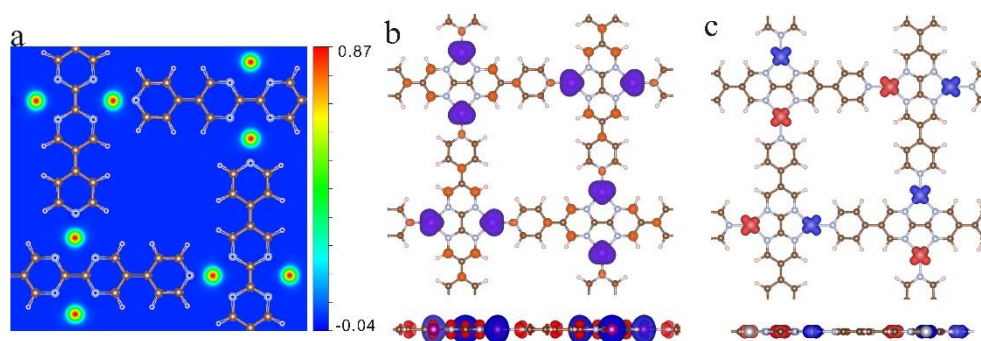


Figure S6. (a) The spin-polarized charge density distribution of Mn-PBP on the plane crossing the Mn atoms. The scale bar unit is e/bohr^3 . The range is from $-0.04 e/\text{bohr}^3$ to $0.87 e/\text{bohr}^3$, which is different from Fig. 3(b) in the main text. Top and side view of spin-polarized charge density distribution of (b) FM Mn-PBP. Top and side view of spin-polarized charge density distribution of (c) AFM Fe-PBP. The purple and red colors represent major and minor spin, respectively and the isosurface value is $0.01 e/\text{\AA}^3$.

5. 2D Ising model for SS lattice

5.1 2D Ising Hamiltonian for SS lattice

The 2D Ising model Hamiltonian for SS lattice could be expressed as follow,

$$E_{total} = E'_0 + E_{mag} = E'_0 + \sum_{\langle i,j \rangle} J_1 \cdot \vec{u}_i \cdot \vec{u}_j + \sum_{\langle l,m \rangle} J_2 \cdot \vec{u}_l \cdot \vec{u}_m \quad (5)$$

Where the E'_0 and E_{mag} represent the total energy without the magnetic contribution and the magnetic contribution, respectively. J_1 and J_2 are the exchange coupling constants for the nearest and second-nearest interactions. \vec{u}_i (\vec{u}_j) and \vec{u}_l (\vec{u}_m) are the spin operators of magnetic moments at neighboring sites i and j (l and m), respectively.

5.2 The calculation of exchange coupling constants J_1 and J_2

Considering there are four TM atoms in each unit cell, the total energy per unit cell with different magnetic configurations can be expressed as follows according to the above model Hamiltonian,

$$E_{FM} = E'_0 + E_{mag} = E'_0 + 2 \cdot J_1 \cdot \vec{u}^2 + 8 \cdot J_2 \cdot \vec{u}^2 \quad (6)$$

$$E_{AFM_Néel} = E'_0 + E_{mag} = E'_0 + 2 \cdot J_1 \cdot \vec{u}^2 - 8 \cdot J_2 \cdot \vec{u}^2 \quad (7)$$

$$E_{AFM_Stripe} = E'_0 + E_{mag} = E'_0 - 2 \cdot J_1 \cdot \vec{u}^2 \quad (8)$$

then coupling constant J_1 and J_2 can be derived,

$$J_1 = \frac{(E_{FM} + E_{AFM_Néel} - 2 \cdot E_{AFM_Stripe})}{8 \cdot \vec{u}^2} \quad (9)$$

$$J_2 = \frac{(E_{FM} - E_{AFM_Néel})}{16 \cdot \vec{u}^2} \quad (10)$$

5.3 Spin wave dispersion of Mn-PBP

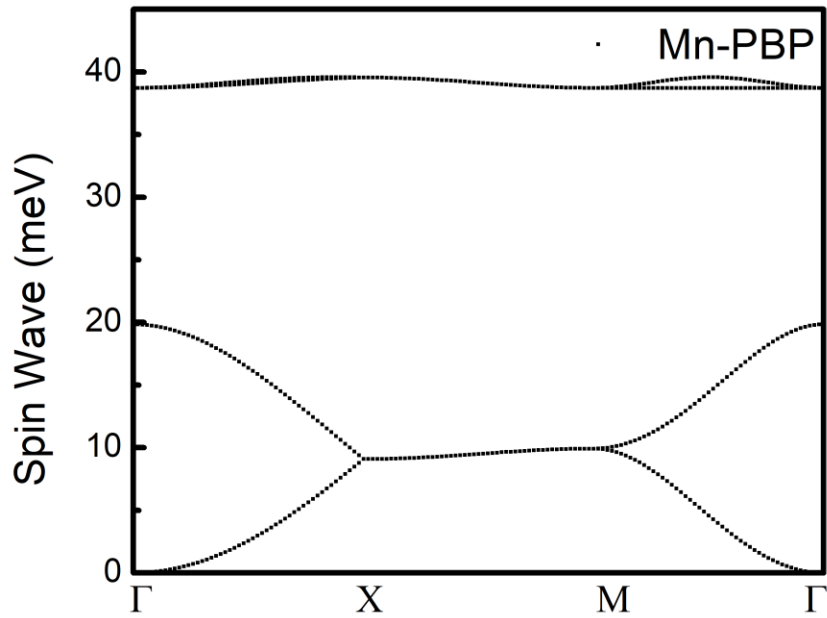


Figure S7. The spin wave dispersion of Mn-PBP is calculated according to the Heisenberg spin model. The Heisenberg exchange between nearest and next-nearest interactions are considered, where the parameters are calculated from the Ising model.

6. The influence of the different effective U

6.1 Magnetic ground state of Mn-PBP with different U_{eff}

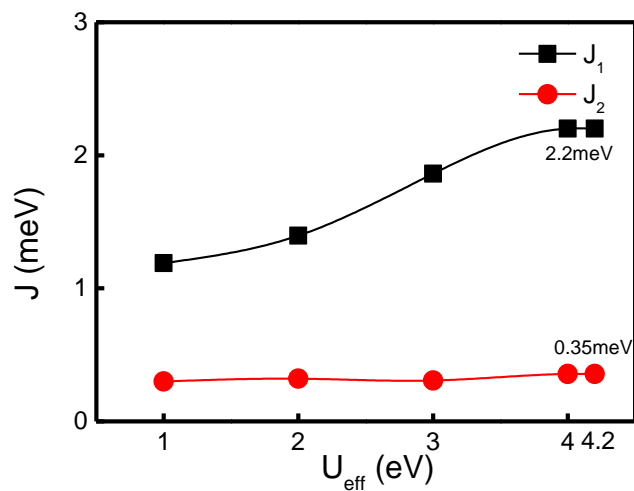


Figure S8. The J of PBP-Mn as a function of the effective U . The black line represents J_1 , and the red line represents J_2 . Note J_1 and J_2 are all negative! Here the absolute values are shown.

6.2 The band structures of Mn-PBP with different U_{eff}

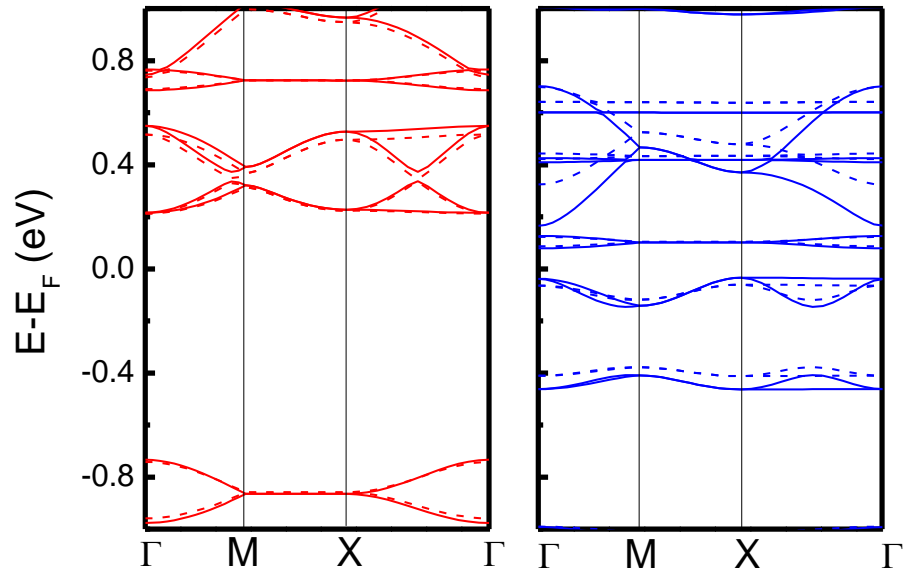


Figure S9. Band structures of Mn-PBP with different U_{eff} . Left panel: spin-down bands (red); Right panel: spin-up bands (blue). The solid lines and dotted lines represent the band structure with $U_{eff} = 3$ eV and $U_{eff} = 4.2$ eV, respectively.

6.3 The simulated Curie temperature of Mn-PBP with different U_{eff}

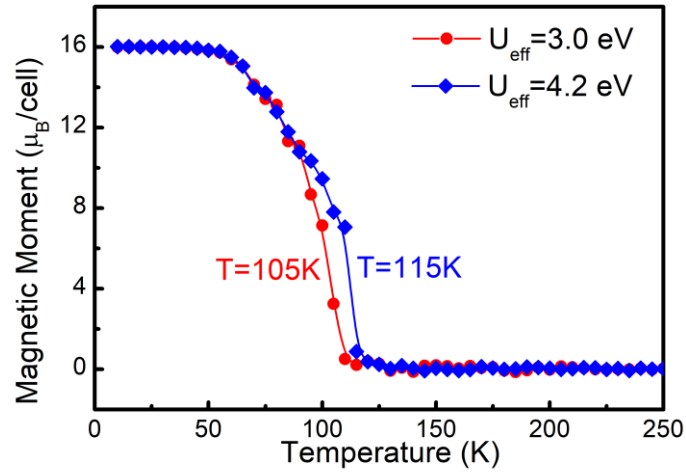


Figure. S10. The average magnetic moment per Mn-PBP unit cell varies with the temperature changes. The red and blue lines are results corresponding to different U_{eff} . The derived Curie temperatures are indicated.

7. Strain effects on the electronic structure of Mn-PBP

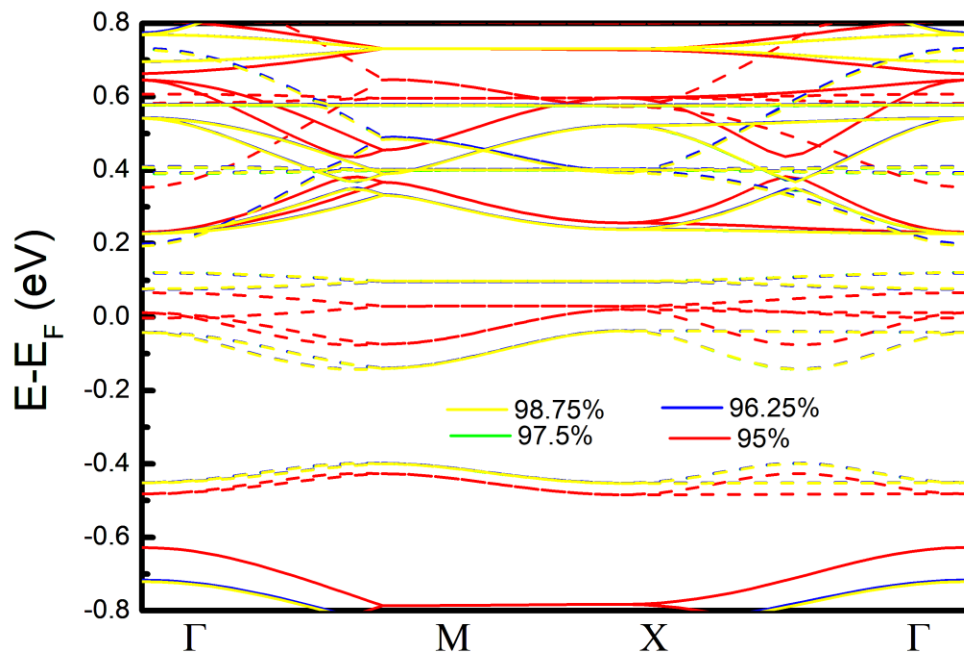


Figure S11. The band structures of Mn-PBP under different biaxial strain. The solid and dotted lines represent the spin-up and spin-down bands, respectively. Different biaxial compressions are applied, and the corresponding lattice parameters are varying from 98.75% to 95% of the original lattice parameter. Obviously, 95% compression could close the spin-down band gap and turn Mn-PBP into a half metal.

8. Magnetic anisotropic energy

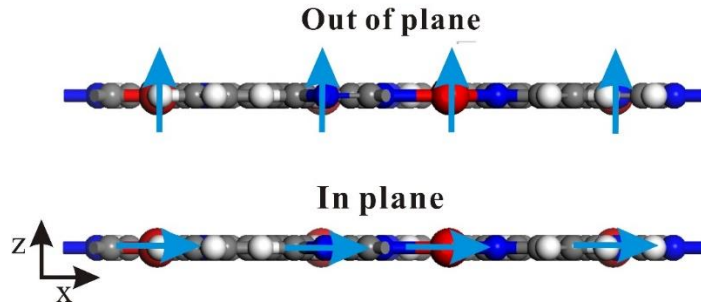


Figure S12. Two typical different spin directions, i.e., out-of-plane and in-plane, for Mn atoms are selected for the calculation of anisotropic energy of Mn-PBP.

Table S2. Total energy of Mn-PBP with two different spin directions (out-of-plane and in-plane). The anisotropic energy is obtained with the value of 0.034meV.

| Spin direction | <i>Out-of-plane</i> | <i>In-plane</i> | <i>Anisotropic energy</i> |
|-------------------|---------------------|-----------------|---------------------------|
| Total energy (eV) | -537.012650 | -537.012616 | 0.000034 |

As for Dzyaloshinskii–Moriya interaction, in Mn-PBP, the nearest magnetic interaction has inversion symmetry, and second nearest interactions are very weak, thereby the Dzyaloshinskii–Moriya interactions can be ignored.

9. Mn-PBP under compression

Unlike 2D materials bonded with covalent bonds, e.g., graphene, the Mn-PBP is bonded with coordination bonds. To analyze whether the buckling exists in our system with compressive strain, supplemental *ab initio* calculations have been done. As the unit cell of Mn-PBP contains more than 70 atoms, a $2 \times 2 \times 1$ supercell (more than 300 atoms) is adopted in our calculation. The structural optimization results show that the structure keeps flat, and even almost the same results can be obtained from a slightly imperfect flat initial structure.

After comparing the relaxed compressed structure with pristine structure, we find that the coordination bonds have more tolerance on compressive strain than covalent bonds. As listed in Table S3, with 95% biaxial compressive strain applied to 2D Mn-PBP, the bond lengths in PBP molecule are only reduced about 1.5% averagely, while the Mn-N bonds lengths are reduced about 6%~7%. As a result, we believe that this 2D MOF bonded with coordination bonds has more tolerance under the compression and the buckling effect should be much weaker than that in purely covalent bonded 2D materials.

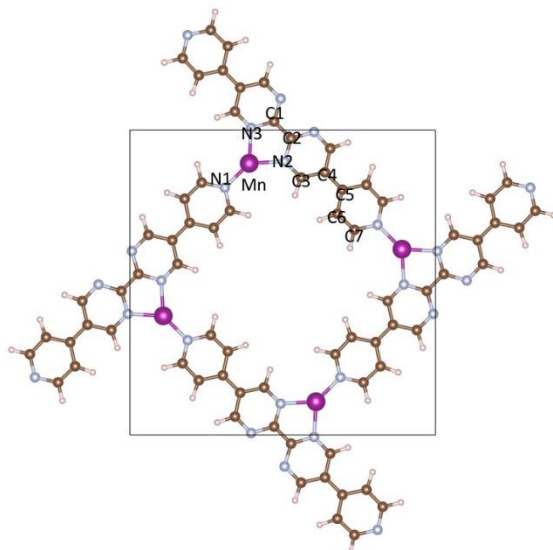


Figure S13. The schematic structure of Mn-PBP with marked atoms.

Table S3. The comparison of the bond length (angstrom) for Mn-PBP framework with 100% (pristine structure) and 95% biaxial compression. The atoms are indicated in Fig. S13.

| strain | C1-C2 | C2-N2 | N2-C3 | C3-C4 | C4-C5 | C5-C6 | C6-C7 | C7-N1 | Mn-N1 | Mn-N2/3 |
|----------------|--------|--------|--------|--------|--------|--------|--------|--------|--------|---------|
| 100% (l_0) | 1.4013 | 1.388 | 1.349 | 1.4237 | 1.4318 | 1.4319 | 1.3715 | 1.3792 | 2.01 | 2.06 |
| 95.% (l) | 1.3937 | 1.3676 | 1.329 | 1.4035 | 1.3895 | 1.4203 | 1.3513 | 1.3605 | 1.865 | 1.938 |
| l/l_0 | 99.46% | 98.53% | 98.52% | 98.58% | 97.05% | 99.19% | 98.53% | 98.64% | 92.79% | 94.01% |

Experimentally, the compression of 2D material is usually realized through applying compression to its substrate. Here, we tested a new model using BN monolayer as the substrate of Mn-PBP, which contains 188 atoms in a unit cell. Then the BN monolayer with a certain strain is fixed to apply 95% compression on Mn-PBP, where only the PBP molecules and Mn atoms are relaxed. The result is shown in Fig. S14. Interestingly, a slight buckling is observed, and all the Mn atoms move downward to approach the BN monolayer, implying the BN layer has attractiveness to Mn atoms. However, after comparing the total energy of different magnetic configurations, we conclude that the ground state of Mn-PBP is still Ferromagnetic (FM). The effects of different substrates on Mn-PBP may be different. Due to the huge calculation cost, we can't make exhaustive study here.

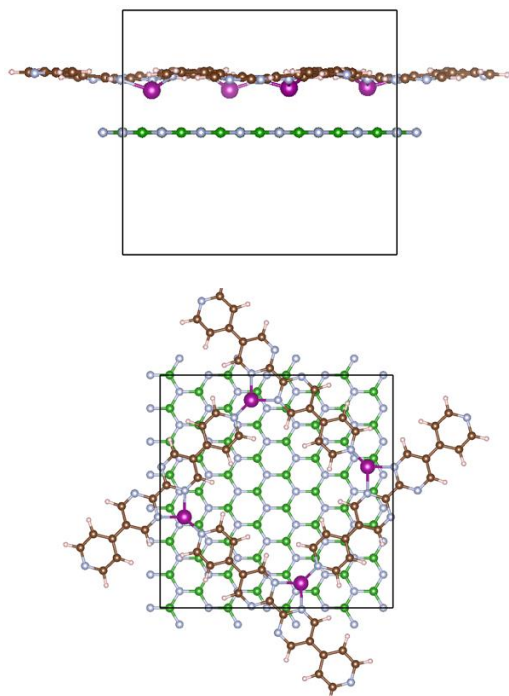


Figure S14. The relaxed structure of Mn-PBP with monolayer BN as the substrate. The top and bottom panels are side view and top view, respectively.

In conclusion, the coordination-bonded Mn-PBP may tolerate larger strain than covalent-bonded 2D materials. Using BN monolayer as the substrate may induce interesting results, but the ground state of Mn-PBP is still FM. The effects of different substrates on MOFs and the interaction mechanism deserve further investigation in future.